7 Novel Approaches to Visual Information Processing in Insects: Case Studies on Neuronal Computations in the Blowfly

Martin Egelhaaf, Jan Grewe, Katja Karmeier
Roland Kern, Rafael Kurtz, and
Anne-Kathrin Warzecha

CONTENTS

7.1 INTRODUCTION

Vision guides behavior in virtually all animals, especially in numerous insects. The array of photoreceptors in the eye typically receives a wildly fluctuating pattern of image flow when the animal moves through its environment. It is the

0-8493-2024-0/05/$0.00+$1.50

task of the brain to interpret this complex spatio–temporal input and to make use of it in guiding behavior. Biological nervous systems outperform existing artificial vision systems with regard to their capabilities to process retinal image flow. Insects make efficient use of visual information, for instance, during the aerobatic chasing maneuvers of male flies in the context of mating behavior (Boeddeker and Egelhaaf, 2003a, 2003b; Boeddeker et al., 2003; Land and Collett, 1974; Wagner, 1986) and the ability of bees to assess, on the basis of visual motion cues, the distance traveled in an unknown environment (Esch and Burns, 1996; Esch et al., 2001; Srinivasan et al., 2000). These extraordinary capabilities are most remarkable given the small number of neurons in insect brains and the astonishing speed with which retinal images are processed.

Because the nervous systems of insects are well amenable to electrophysiological and imaging techniques under *in vivo* conditions, insects have served for many years as model systems for analyzing the processing of retinal image flow (review: Egelhaaf and Kern, 2002). Novel experimental approaches at both the behavioral and the neuronal levels, as well as new techniques for data analysis, are beginning to unveil the mechanisms underlying the amazing visual capabilities of insects (see also Chapter 1, Chapter 2, Chapter 6, and Chapter 8). In particular, blowflies have been used as a model system for understanding how visual motion information is processed (Borst and Haag, 2002; Egelhaaf et al., 2002; Kurtz and Egelhaaf, 2003). Results on blowflies will, therefore, form the basis of this review, but wherever possible we also refer to the work done on other insect groups.

Visual motion has been shown to play an important role in behavioral control in blowflies. Examples are visual course control, landing behavior, and object–background discrimination. In mediating these behavioral maneuvers, the nervous system of blowflies relies on extracting behaviorally relevant information from the continually changing brightness patterns that are generated on the eyes during locomotion. This so-called optic flow contains information both about the direction and speed of the animal's self-motion and about the environmental layout (Koenderink, 1986; Lappe, 2000). The behavioral significance of motion vision in blowflies and other insects is reflected in an abundance of motion-sensitive neurons in their visual system (reviews: Wehner, 1981; Hausen, 1981; Hausen and Egelhaaf, 1989; Rind and Simmons, 1999; see also Chapter 8).

An ensemble of large visual interneurons, the so-called tangential cells (TCs), in the blowfly's third visual neuropil (the lobula complex) has been characterized in particular detail and is assumed to play a key role in processing visual motion information in the context of visually guided behavior. Most TCs receive their main input from two sets of retinotopically organized, local, motion-sensitive interneurons with opposite preferred directions. As a consequence, they respond in a directionally selective manner to motion in large parts of the visual field (reviews: Borst and Haag, 2002; Egelhaaf and Warzecha, 1999; Egelhaaf et al., 2002; Hausen and Egelhaaf, 1989). Neither the preferred directions of motion of TCs nor their motion sensitivities are homogeneous, but these change in a systematic way across the visual field. These intricate receptive field structures, which represent a phylogenetic adaptation rather than the outcome of sensory experience (Karmeier et al., 2001), suggest that TCs are tuned to certain patterns of optic flow, as seen in the blowfly during

specific types of self-motion (Hengstenberg, 1982; Krapp and Hengstenberg, 1996; Krapp et al., 2001).

Some TCs receive, either exclusively or in addition to their retinotopic input, excitatory or inhibitory input from other TCs (Egelhaaf et al., 1993; Haag and Borst, 2001, 2002; Hausen and Egelhaaf, 1989; Horstmann et al., 2000; Warzecha et al., 1993). This input is assumed to enhance the selectivity of TCs for optic flow. As a consequence, some TCs respond best during coherent wide-field motion, as may occur while an animal turns around a particular body axis (reviews: Egelhaaf and Warzecha, 1999; Egelhaaf et al., 2002; Hausen, 1981; Hausen and Egelhaaf, 1989; Krapp, 2000). Others respond best to object motion, as may occur while the animal pursues a moving target or passes a stationary object in its environment (Collett, 1971; Egelhaaf, 1985a, 1985b; Gauck and Borst, 1999; Gilbert and Strausfeld, 1991; Kimmerle and Egelhaaf, 2000a, 2000b; Olberg, 1981, 1986; Olberg and Pinter, 1990).

By employing novel approaches, three different but related aspects of motion computation have been addressed in recent years:

1. Visual information processing in small neuronal networks
2. The reliability of encoding of visual motion by neuronal populations
3. The neuronal representation of natural optic flow

The merits and limitations of these novel approaches will be summarized in the following pages, and we discuss how they have contributed to our understanding of how behaviorally relevant visual information is processed in the insect brain.

7.2 METHODS FOR ANALYZING VISUAL INFORMATION PROCESSING IN SMALL NEURAL NETWORKS

From a methodological point of view, the intricate network of TCs is a particularly advantageous model system to analyze the cellular basis of neural computation under *in vivo* conditions. Dendritic information processing and synaptic transmission can be analyzed by electrophysiological and optical recording techniques while the animal is stimulated by its natural visual input. Imaging of the intracellular activity distribution with calcium-sensitive dyes (see also Chapter 6 and Chapter 13) is feasible in the virtually intact brain, because TCs arborize in a plane almost parallel and close to the brain surface. In this way, it has not only been possible to unravel major parts of the neuronal circuitry at this level of the visual pathway, but also to elucidate how these neuronal circuits process information under their normal operating conditions.

7.2.1 Identifying Neural Networks

Dual electrophysiological recordings (see also Chapter 12 and Chapter 14) have been successfully applied to analyze synaptic connections within a neuronal circuit and are still the technique of choice, because they provide a means of establishing

synaptic connections between two cells and of characterizing their functional properties. For instance, one of the cells of the so-called horizontal system, the HSE cell (horizontal system equatorial cell), was shown using this method to receive input from two TCs that reside in the contralateral half of the visual system. Both are excited by back-to-front motion. Owing to its ipsilateral retinotopic input, HSE is excited by front-to-back motion, so it can be expected to respond best to wide-field motion as is generated on the eyes when the animal turns about its vertical axis (Figure 7.1) (Horstmann et al., 2000; Krapp et al., 2001).

Recently, two other experimental approaches were employed for network analysis. These approaches allow us to establish synaptic connectivity without requiring simultaneous recording from two cells. The presumptive presynaptic neuron is recorded intracellularly after the presumed postsynaptic cell was intracellularly injected with an activity-dependent fluorescent dye (e.g., a calcium-sensitive dye such as fura 2, calcium-green, or Oregon-green).[14] Synaptic connectivity is established by depolarizing the presynaptic cell by current injection via the recording electrode and monitoring the resulting fluorescence changes in the postsynaptic cell (Haag and Borst, 2001, 2002, 2003). Synaptic network interactions have been further established by the so-called fill-and-kill technique (Farrow et al., 2003; Miller and Selverston, 1979; Warzecha et al., 1993). The presynaptic cell is injected with a fluorescent dye, 6-carboxy-fluorescein,[26] which becomes phototoxic after laser illumination. After photoablation of the presynaptic neuron, the functional consequences for the postsynaptic cell can be characterized. Using this method, it was established that a particular TC, a so-called *figure detection neuron* (FD1), is inhibited by one of the GABAergic *centrifugal horizontal cells* (CH cells) (Figure 7.2) (Warzecha et al., 1993). As a consequence of this inhibition, the FD1 neuron responds best to object motion but shows little activity during wide-field motion (Figure 7.2b). This circuit was further analyzed by photoablation of neurons that are presynaptic to the CH cells: CH cells receive their main ipsilateral motion input not from retinotopic

FIGURE 7.1 **a**: Schematic of synaptic input organization of the HSE cell in the right half of the brain. It receives input from many retinotopically organized local motion-sensitive input elements (indicated by thin lines) in the ipsilateral visual field. Information about back-to-front motion in the contralateral visual field is mediated by the H1 and the H2 cell. The H2 cell contacts the HSE cell close to its output terminal; the H1 cell is likely to make a multitude of synaptic connections with its extended terminal region on the dendritic tree of the HSE cell. Gray arrows indicate the direction of signal flow in the cells. The light gray insets illustrate, seen from above, the fly looking at various motion stimuli and indicate the preferred directions of motion of the different cells. The graphs (below) display the EPSPs recorded in the HSE cell as evoked by the H1 and the H2 cell, respectively. Vertical arrows mark the occurrence of the H1 and H2 spike, respectively. **b**: Time courses of responses of the HSE cell in the right half of the brain to rotational optic flow, as well as the corresponding monocular components. The arrows indicate front-to-back and back-to-front motion in the right and left visual field, respectively. Although the cell mainly shows graded depolarizations during ipsilateral front-to-back motion (first trace), there are many response transients during contralateral back-to-front motion (second trace) and clockwise rotational optic flow (third trace). The duration of motion is indicated by the black horizontal bar. (From Horstmann, W. et al., *Eur. J. Neurosci.* **12**:2157–2165, 2000. With permission.)

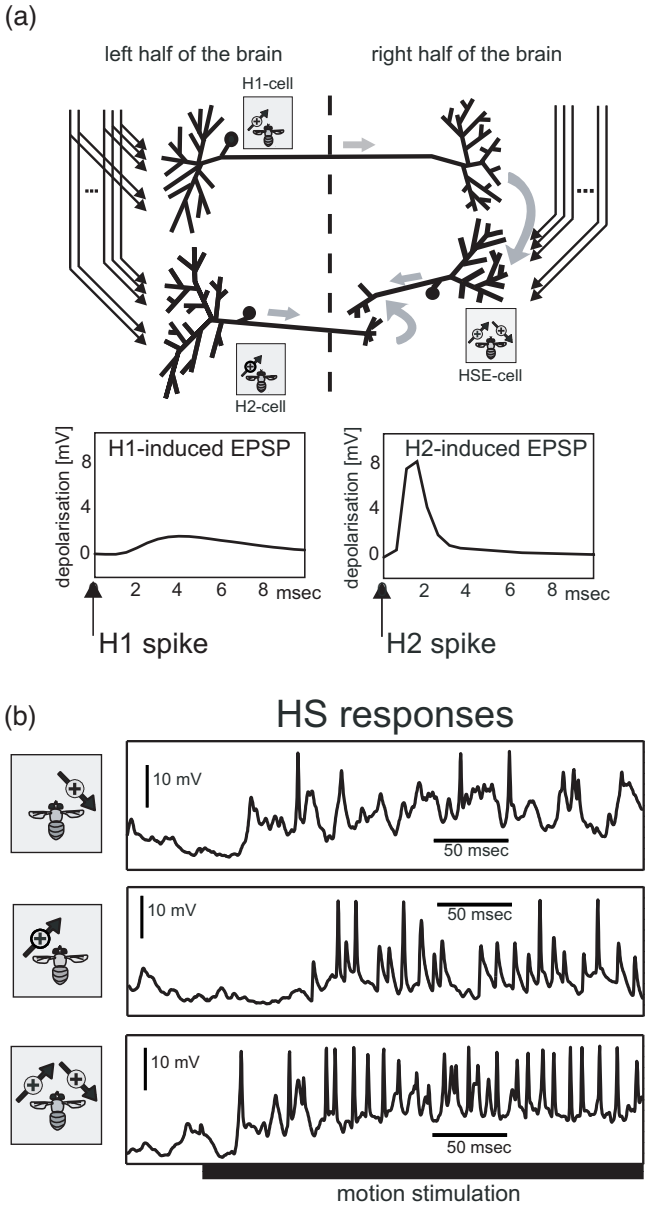

FIGURE 7.1

small-field elements, as is the case for most other TCs, but via dendro–dendritic interactions from the HS cells. After laser ablation of HS cells, the CH cells could no longer respond to motion in front of the ipsilateral eye, and only responses to motion in the contralateral visual field remained (Farrow et al., 2003).

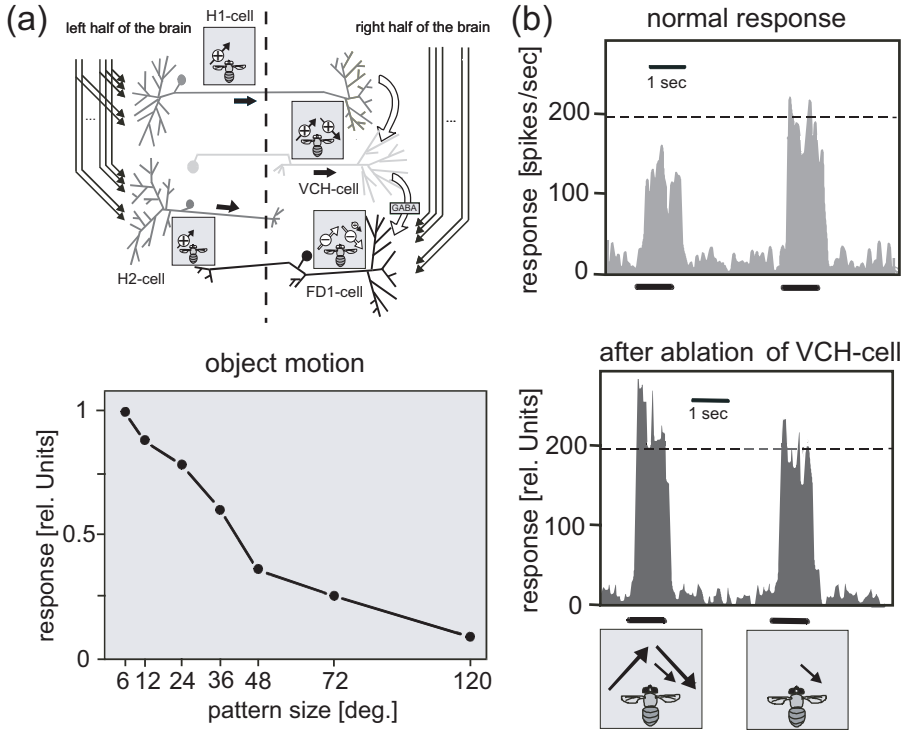

FIGURE 7.2 **a**: Left: Schematic of input organization of one of the figure detection cells, the FD1 cell. It receives input from many retinotopically organized local motion sensitive input elements (indicated by thin lines) in the ipsilateral visual field. It is inhibited via GABAergic synapses by one of the CH cells, the VCH cell. The VCH cell receives excitatory input from the contralateral eye via the H1 and the H2 cell. Black arrows indicate the direction of signal flow within the cells. Insets illustrate, seen from above, the fly looking at various motion stimuli and indicate the preferred directions of motion (black arrows) of the different cells or of the inhibitory input of the FD1 cell (open arrows). Bottom plot: Response of the FD1 cell as a function of pattern size, illustrating that it is most sensitive to the motion of a small pattern. (From Egelhaaf, *Biol. Cybern.* **52**:195–209,1985a. With permission.) **b**: Spike frequency histogram of responses of FD1 cell to wide-field and small-field motion (indicated in the insets below the diagrams) before and after photoablation of the ipsilateral VCH cell. Horizontal bars below the responses indicate the duration of motion. Arrows in insets symbolize the size and direction of the moving pattern. Dotted horizontal lines indicate mean response amplitudes during small-field motion. (From Warzecha, A-K. et al., *J. Neurophysiol.* **69**:329–339, 1993. With permission.)

By applying these approaches to neuronal network analysis, it has been possible to unravel major parts of the wiring diagram of the intricate network of TCs in the blowfly's third visual neuropil. The interactions that take place within the network are thought to play an important role in tuning TCs to particular types of optic flow, as are generated on the eyes when the animal turns around a particular body axis or passes a nearby object in front of a more distant background. The network

interactions comprise heterolateral interactions, recurrent inhibitory interactions, and feed-forward inhibition. For instance, the HSE cells are major output elements of the visual system. In parallel they act, via dendro–dendritic synapses, as excitatory input elements of the CH cells, the inhibitory inputs of the object-motion sensitive FD1 cell (see previous), as well as of an excitatory heterolateral element, the H1 cell (see Chapter 8). The latter neuron in turn excites, among other cells, the contralateral HSE cell and the contralateral CH cells (Figure 7.3). Modeling is required to infer the functional significance of this intricate connection pattern.

7.2.2 Computational Properties of Synaptic Interactions

Understanding the computational properties of a neuronal network requires knowledge about details of the neuronal wiring scheme, but also about the functional properties of the synaptic connections. In general, synapses are particularly important sites of cellular information processing, because they may have peculiar nonlinear properties and may even change their transmission properties depending on their activation history (Fortune and Rose, 2001; Juusola et al., 1996; Paulsen and Sejnowski, 2000; Sabatini and Regehr, 1999; Simmons, 2002; Thomson, 2000).

Meaningful representations of optic flow are often only achieved by specific synaptic interactions between TCs (see previous section). To be beneficial, these synaptic interactions must be carefully adjusted to the natural operating range of the system. Otherwise, synaptic transmission may severely distort the information being transmitted. This hazard is particularly daunting because synaptic transmission is inherently noisy and the underlying biophysical processes have been found in many

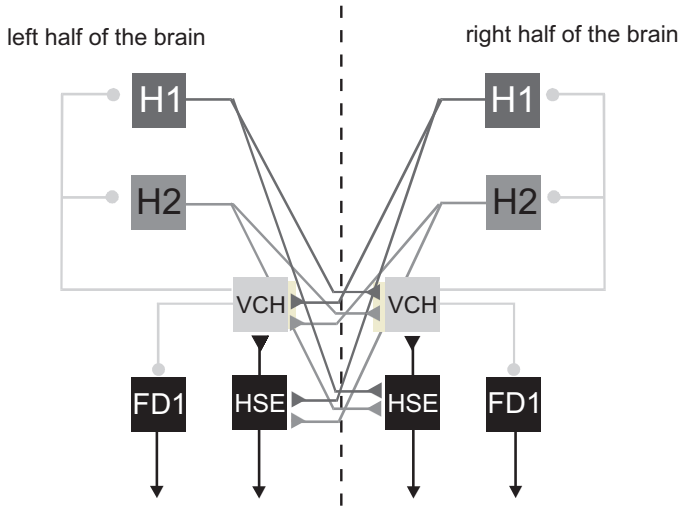

FIGURE 7.3 Relationship of the two neural circuits sketched in Figure 7.1a and Figure 7.2, tuning blowfly tangential cells either to coherent wide-field motion or object motion, respectively. The cells are indicated by boxes. Excitatory and inhibitory synapses are indicated by triangles and circles, respectively. Note the reciprocal recurrent inhibitory connections between neurons in both halves of the visual system.

systems to be intrinsically nonlinear. Moreover, the transformation of the postsynaptic potential into spike activity may also be nonlinear. Combined electrophysiological and *in vivo* optical imaging experiments were performed in the blowfly to analyze the relationship between the activity of a given presynaptic TC and the spike rate of its postsynaptic target in the contralateral visual system. It was found that the entire range of presynaptic depolarization levels that can be elicited by motion in the "preferred direction" is transformed approximately linearly into the postsynaptic spike rate (Figure 7.4) (Kurtz et al., 2001). This is surprising, especially given the potential nonlinearities mentioned earlier. Linearity characterizes the transmission of membrane potential fluctuations up to frequencies of 10 Hz (see ~~below~~; Figure 7.6B) (Warzecha et al., 2003). Thus, the linear synaptic regime covers most of the dynamic range within which visual motion information is transmitted with high gain (Haag and Borst, 1997; Warzecha et al., 1998). In addition to slow graded membrane potential changes, rapid presynaptic depolarizations, such as spikes, are also transmitted reliably at this synapse (Warzecha et al., 2003). As a consequence of the computational properties of the analyzed synapse, visual motion information is transmitted largely undistorted to the contralateral visual system. This ensures that the characteristic dependence of neural responses on stimulus parameters such as velocity or contrast is not affected by the intervening synapse.

AU: Pls specify where (which section).

Presynaptic transmitter release is thought to be controlled by changes in the presynaptic calcium concentration. Therefore, presynaptic calcium concentration changes were monitored after the presynaptic cell was injected with a calcium-sensitive fluorescent dye. This allows us to monitor the time-dependent changes in calcium concentration in different parts of the axon terminal (Figure 7.4a). Interestingly, a linear relationship was found between presynaptic depolarization as is induced during preferred direction motion and the presynaptic calcium concentration. Moreover, the postsynaptic spike rate was also linearly related to presynaptic calcium concentration increases (Figure 7.4b) (Kurtz et al., 2001). Although these findings are in accordance with the overall characteristics of synaptic transmission, one should be careful in interpreting the measured presynaptic calcium signals to reflect precisely the calcium concentration that is relevant in the control of transmitter release: with conventional *in vivo* imaging techniques, only the bulk calcium concentration changes within presynaptic arborizations can be monitored (see also Chapter 13). In contrast, the calcium concentration changes that are relevant for transmitter release are likely to be regulated very close to the presynaptic membrane (review: Neher, 1998).

Because conclusions on the role of calcium in synaptic transmission are critically dependent on the exact determination of presynaptic calcium changes, two new technical approaches are currently tested. First, to overcome spatial resolution limits of conventional intracellular imaging, two-photon laser scanning fluorescence microscopy has recently been adjusted for *in vivo* analysis of presynaptic calcium concentration changes at high spatial and temporal resolution (Kalb et al., 2004). Second, to relate presynaptic calcium concentration changes and postsynaptic activity in a more systematic way than is possible by visual stimulation, the flash-photolysis technique is used to release calcium in the presynaptic neuron. Here, the presynaptic neuron is injected with a photolabile cal-

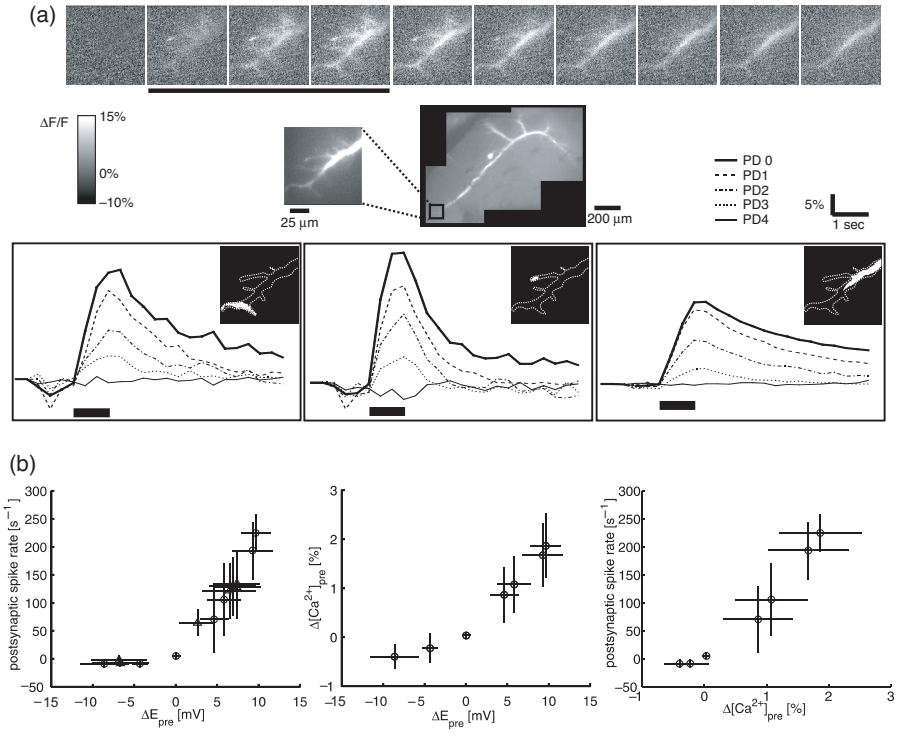

FIGURE 7.4 Transmission of optic flow information between a pair of TCs. **a**: Upper diagram: Presynaptic calcium accumulation in a VS cell filled with a calcium-sensitive fluorescent dye (raw fluorescence images of the entire cell and of the presynaptic region, left diagrams) during presentation of preferred direction motion (black horizontal bar). White and light gray values in the images correspond to increases in calcium concentration (measured as relative change in fluorescence: ΔF/F). Bottom diagrams: Time courses of presynaptic calcium concentration changes in three regions of the axon terminal (indicated in the insets) for variable stimulus strengths (different line types). The insets correspond to the terminal region as seen on the left raw fluorescence image. **b**: Linearity of the transfer of preferred direction motion. Left: Postsynaptic spike rate (relative to resting activity) is plotted vs. the presynaptic membrane potential change (ΔE_{pre}) for visual stimuli of variable strengths, moving either in the preferred direction (positive ΔE_{pre} values) or in the null direction (negative ΔE_{pre} values). The gain of signal transfer is about constant for the entire range of visually induced excitations, resulting in a linear relationship between presynaptic potential and postsynaptic spike rate upon motion in the preferred direction. A rectification is prominent for null direction motion. Linear dependencies for preferred direction motion are also present in the relationship between changes in presynaptic calcium and in presynaptic membrane potential (middle) and in that between postsynaptic spike rate and changes in presynaptic calcium (right). (From Kurtz, R. et al., *J. Neurosci.* **21**:6957–6966, 2001. With permission.)

cium cage (BAPTA-1 hexapotassium salt or NP-EGTA tetrapotassium salt).[14] This compound is loaded with calcium that is rapidly released upon illumination of the preparation with a brief, high-intensity flash of the appropriate wavelength (Kurtz, 2004). These techniques are currently adjusted for their use in the intact

fly brain to unravel the role of calcium in synaptic transmission — and thus in neuronal processing of optic flow information.

7.3 APPROACHES TO STUDY THE RELIABILITY OF ENCODING VISUAL MOTION INFORMATION

By simply looking at the architecture of neuronal circuits, it is hard to infer how reliably they extract the relevant information under normal behavioral conditions. One reason for this is the large variability of neuronal responses, even if these are evoked by repeated presentation of the same stimulus. Although the across-trial variance of the spike count in fly TCs is smaller than in motion-sensitive neurons in the primate cortex (see e.g., Barberini et al., 2000; de Ruyter van Steveninck et al., 1997; Warzecha and Egelhaaf, 1999; Warzecha et al., 2000), it is hard to deduce from individual spike trains the extent to which variations in the interspike interval are caused by the stimulus or by sources that are not time-locked to the stimulus (*noise*). Neuronal response variability limits the timescale on which time-varying optic flow can be conveyed.

The performance of a neuron in real time can only be understood by scrutinizing individual response traces, not on the basis of ensemble averages. This requires assessing the variability in a quantitative way by appropriate statistical measures. The spike count variance across trials is the most straightforward measure of neuronal variability. However, this measure does not take into account the time course of neuronal activities that may be particularly important when analyzing responses to time-varying stimuli. In the following section, we briefly summarize some methods to quantify the variability of time-varying neuronal data and to analyze the timescale on which sensory information is encoded by the nervous system.

To understand the specificity of sensory coding, the analysis must be extended from individual neurons to populations of neurons that all respond to somewhat different aspects of the stimulus (see Chapter 14). The significance of population coding can be analyzed particularly well on blowfly TCs, because the neurons comprising the population are largely known and are accessible to experimental analysis. Elaborate theoretical tools have been developed to assess (i) how well different optic flow patterns, as induced by the animal's self-motion, can be distinguished from each other and (ii) how specifically these optic flow patterns are encoded on the basis of the population responses. Some of these theoretical tools will be summarized with regard to optic flow encoding by fly TCs.

7.3.1 Reliability of Neural Coding by Individual Nerve Cells

There are various measures to quantify the reliability of neuronal responses to time-varying stimuli. If repetitive stimulation with a given stimulus led always to identical neuronal responses, the timing of spikes would be determined exclusively by the stimulus. Obviously, sensory neurons do not respond with absolute accuracy, and the timing of spikes varies considerably from trial to trial. Thus, it is most likely that spike timing depends on noise sources, such as the stochastic absorption of

photons by the photoreceptors or the stochastic nature of transmitter release at synapses and the subsequent opening and closing of ionic channels.

Several approaches to quantify neuronal variability are based on information theory (reviews: Borst and Theunissen, 1999; Rieke et al., 1997). Applying these measures allows us to analyze how much information about the stimulus is encoded by a neuron. Information theory implies that a stimulus that assumes many states contains more information than a stimulus assuming, for instance, only two states. Moreover, the information content of a stimulus depends also on the probability of the different stimulus states. Accordingly, the information conveyed by a neuron depends on the probability distribution of the neuronal response levels. The mutual information between stimulus and response specifies how much information about the different states of the stimulus is represented by the neural response (Figure 7.5). The mutual information between stimulus and response is constrained by the variability of neuronal responses upon repetitive presentation of a given stimulus. The mutual information can be determined from the relationship of the probability distribution of response levels when a particular stimulus is presented (conditional probability) and the overall probability distribution of the different responses levels obtained for all stimulus conditions (Figure 7.5).

Although, in principle, this procedure for determining the mutual information is simple, it can be applied in practice only with some difficulty (Borst and Theunissen, 1999). A major reason for this difficulty is that the different stimulus conditions and the different response states need to be defined explicitly. This may be feasible for simple stimuli (e.g., a pattern that moves only to the left or to the right, or a moving pattern whose orientation is varied in discrete steps), but is hardly possible for complex time-dependent stimuli. Therefore, more practical approaches to quantify stimulus–response relationships have been developed that simplify matters but, as a trade-off, are based on certain assumptions about the properties of the stimuli or of the neuronal responses. One type of approach, *linear reconstruction techniques*, will be summarized briefly without going into formal details (for details, see Bendat and Piersol, 2000; Borst and Theunissen, 1999; Marmarelis and Marmarelis, 1978; Rieke et al., 1997).

Here, the neuronal encoding of a signal is not quantified on the basis of probability distributions of stimulus conditions and response levels, but by relating the measured responses to the output of an encoding model, that is, a model that accounts for sensory information processing in formal terms. From a formal point of view, the simplest encoding model is a linear one. The optimal linear model that allows one to estimate a time-dependent signal from another signal can be determined by the so-called *reverse reconstruction approach* (review: Rieke et al., 1997) (Figure 7.6a). This approach has frequently been applied to sensory systems, including blowfly TCs, to investigate how well stimulus velocity can be estimated on the basis of neuronal responses (Bialek et al., 1991; Haag and Borst, 1997, 1998). It was shown that time-dependent stimulus velocity is linearly encoded by blowfly TCs as long as pattern velocity and the velocity changes are relatively small. Otherwise, acceleration and higher-order temporal derivatives play an increasingly large role in shaping the time course of the motion response (Egelhaaf and Reichardt, 1987; Haag and Borst, 1997). Recently, the reverse reconstruction approach has also been applied

(a)

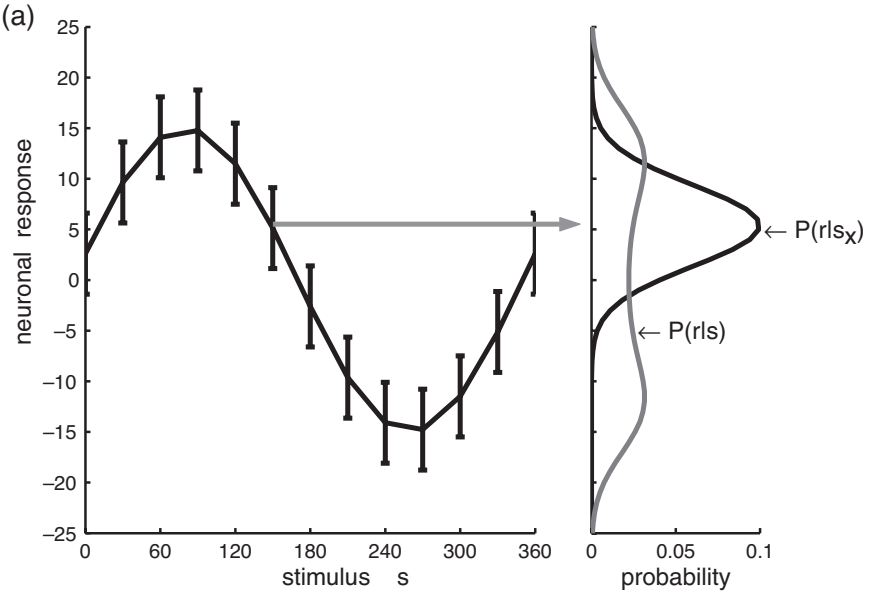

(b)

$p(r)$	probability distribution of the neural response to any stimulus
$p(s_x)$	probability that the stimulus takes the value s_x
$p(r\|s_x)$	probability of neural responses when the stimulus s_x is presented (conditional probability)

Information about a particular stimulus s_x

$$I_{s_x} = \sum p(r|s_x) \log_2 (p(r|s_x) / p(r))$$

Average mutual information obtained from all stimulus conditions:

$$I_s = \sum\sum p(s_x)\, p(r|s_x) \log_2 (p(r|s_x) / p(r))$$

FIGURE 7.5 Information transmitted by a neuron about an input signal (mutual information). **a**: Simulated tuning curve for a range a stimuli. The mean responses and standard deviations are shown as can be measured experimentally. The information conveyed by the neuron depends on the probability distribution of the response amplitudes. The more the probability distributions of responses to particular stimuli $p(r|s_x)$ deviate from the overall response distribution that is obtained for all stimuli p(r), the better the different stimuli can be distinguished on the basis of the neuronal responses and the higher mutual information. **b**: Definition of mutual information and explanation of symbols. The mutual information between stimulus and response can be determined from the relationship of the probability distribution of response levels when a particular stimulus is presented (conditional probability) and the overall probability distribution of the different responses levels that is obtained for all stimulus conditions.

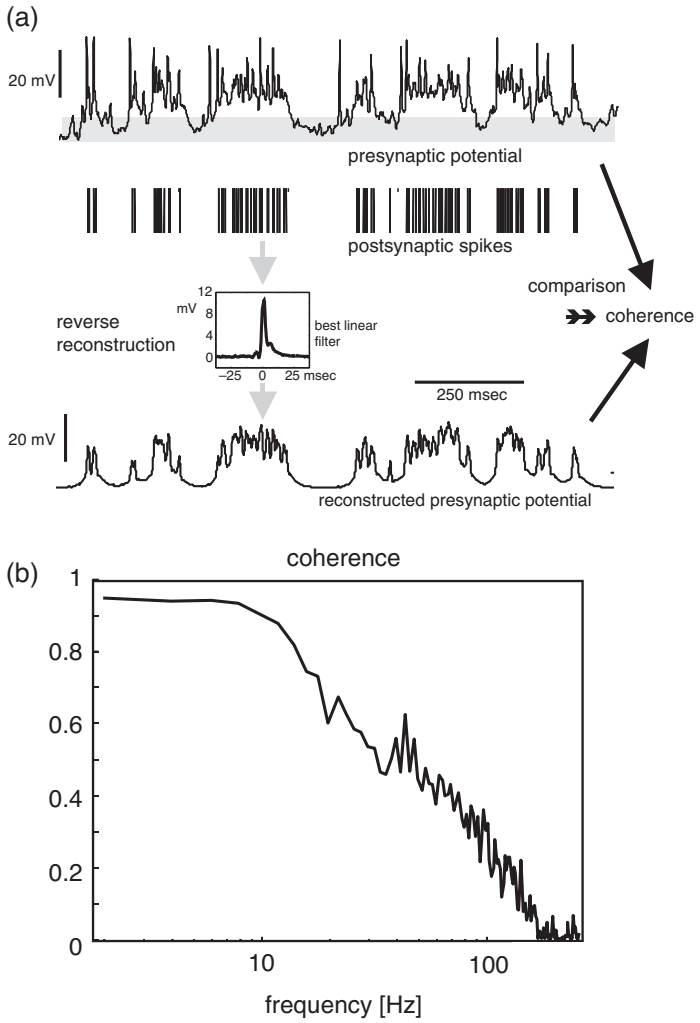

FIGURE 7.6 Reverse reconstruction of the time-dependent presynaptic potential from postsynaptic spike trains. **a**: Schematic outline of the procedure. The linear filter is determined that, when convolved with the postsynaptic spike train, leads to the best estimate of the presynaptic potential. Hyperpolarizations of the presynaptic neuron do not have much effect on the activity of the postsynaptic cell (due to the low postsynaptic resting activity). Therefore, the presynaptic potential was rectified at the resting potential of each response trace and was then used for the reconstruction. The part of the response that was rectified is marked by the shaded bar. The coherence function was determined as a measure of the similarity between the recorded and the estimated presynaptic membrane potential traces. **b**: Coherence determined for a cell pair analyzed with random velocity fluctuations. Coherence values close to 1 for frequencies up to 10 Hz indicate that the system can be regarded as very reliable and approximately linear in this frequency range. (Data from Warzecha, A-K. et al., *Neurosci.* **119**:1103–1112, 2003. With permission.)

to relate the time-dependent postsynaptic signal to the corresponding presynaptic input (Figure 7.6a). The results of these experiments have already been summarized earlier (Warzecha et al., 2003).

The similarity between the responses of the encoding model and the experimentally obtained responses can be determined on the basis of the so-called coherence function, which relates two time-dependent signals as a function of their frequency components (Bendat and Piersol, 2000; van Hateren and Snippe, 2001). In technical terms, the coherence function is the normalized power spectrum of the cross-correlation function between the two time-dependent signals. It varies between 0 (i.e., both signals are unrelated) and 1 (i.e., both signals can be linearly transformed into each other) (Figure 7.6b). There is one ambiguity with the coherence function, which is that a coherence value smaller than 1 can arise from two nonexclusive sources. First, it can be due to inherent noise in the neural pathway, and thus arise from the variability in the neural responses. Second, the neural responses and the responses predicted on the basis of the encoding model are not linearly related. To account for the noise in encoding the stimulus, the so-called expected coherence can be assessed (Haag and Borst, 1998; van Hateren and Snippe, 2001). The expected coherence is determined by calculating the coherence function between the stimulus-induced response component (i.e., the ensemble average of a sufficiently large number of individual responses to the same input) and the individual responses. The expected coherence is related to the signal-to-noise ratio of the neuron (Haag and Borst, 1998; van Hateren and Snippe, 2001). The expected coherence represents the upper limit, given neuronal variability, of what can be maximally expected to be encoded even if a perfect encoding model were available.

The reliability of neural encoding has recently been addressed on the basis of another type of approach to assess the similarity of neural responses. In the context of blowfly motion vision, this approach has been applied to pinpointing the dominating noise source in the visual motion pathway. Here, the similarity of neural responses to a given stimulus is related to the similarity of response traces evoked by different stimuli. The similarity of spike trains can be determined in two ways. The first approach compares spike trains by calculating the minimal costs of transforming one spike train into another (Victor and Purpura, 1996). The transformation is done by either deleting, inserting, or temporally shifting single spikes. Each of these procedures is linked to defined costs (Figure 7.7a,b). By varying the costs for shifting a spike relative to inserting or deleting one, the temporal resolution of the procedure is changed. The second approach to determine similarity calculates the distance between two spike trains that are smoothed by temporal filtering. The distance is given by the square root of the squared differences between the smoothed spike trains (Kretzberg et al., 2001b). Changing the filter width leads to a varying temporal resolution of the procedure.

Both these approaches to determine the similarity of neural responses were used in a blowfly TC to test whether the timing of spikes elicited by visual motion is determined by photon noise, as was proposed in earlier studies (Borst and Haag, 2001; Lewen et al., 2001), or by noise inherent in the nervous system. Simulating photon noise by random brightness fluctuations of moving dots allowed us to show that the reliability of spike timing is dominated by noise intrinsic to the nervous system (Figure 7.7c) (Grewe et al., 2003).

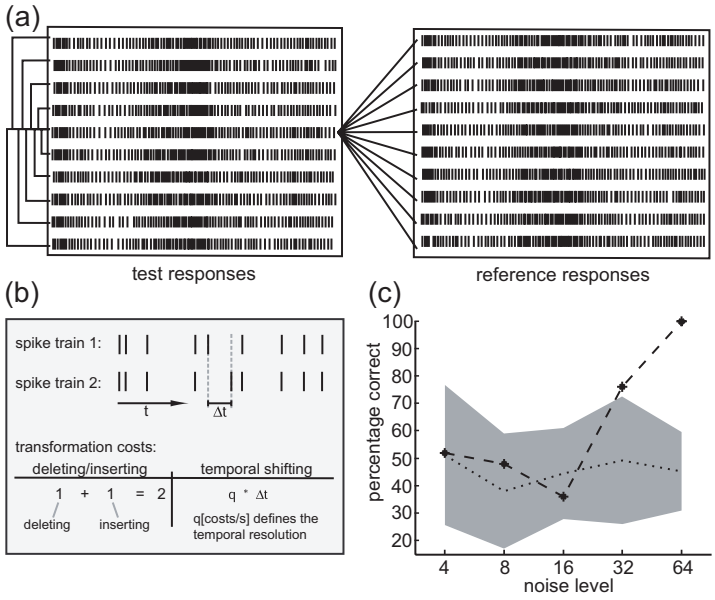

FIGURE 7.7 Similarity of spike trains as evoked by motion stimuli superimposed by variable noise. **a**: The raster plot shows sections out of the spike responses of a blowfly TC (the H1 cell) to a reference and a test stimulus. Both stimuli consisted of the same pattern of ten randomly positioned dots that were moved at a constant velocity in the cell's preferred direction. The dots were superimposed by random luminance fluctuations (noise). These were the same for each presentation of the reference stimulus, but differed, although they had the same statistical properties, for each presentation of the test stimulus (for details, see Grewe et al., 2003). A common spike pattern can be seen in all responses, despite differences in timing of individual spikes. The way of analyzing whether the temporal structure of the reference responses are more similar to each other than to the test responses is sketched by the lines connecting the highlighted reference response and all other reference and test responses. **b**: The similarity between two spike trains is defined as the inverse of the minimal costs of transforming one spike train into another one (Victor and Purpura, 1996). The transformation is done by either deleting, inserting, or temporally shifting single spikes. Deleting or inserting single spikes has the cost of 1. The cost of a temporal shift (q per second) is variable and determines the temporal resolution of the measure. For example, a q value of 200 equals a temporal resolution of 10 msec: for this time-scale spikes in two response traces are considered nearly coincident if a given spike in one of the spike trains is shifted by less than ±10 msec with respect to the corresponding spike in the other spike train. As long as this condition is met, it is "cheaper" to adjust the spikes temporally in the two spike trains by shifting than it is by deleting and inserting one of them. **c**: The pairs of mean similarities, of each reference response to all test responses, and of each reference response to all other reference responses are attributed either to the reference or the test stimulus. Assuming that the reference responses are more similar to each other than to the test responses, the larger similarity value was assigned to the reference response. The percentage of correct decisions is plotted as a function of added noise level. The shaded area represents the domain of uncertainty (see Grewe et al., 2003, for details). Discrimination performances falling into this range are likely to be a consequence of chance. A significant effect of the added noise on the responses can be assumed if the actual percentage-correct value is outside the domain of uncertainty. (From Grewe, J. et al., *J. Neurosci.* **23**:10776–10783, 2003. With permission.)

~~These results are~~ in accordance with findings of earlier studies based on dual recordings of TCs with largely overlapping receptive fields and a correlation analysis of their spike activity. Although the first spike after a rapid change in the direction of motion may be precisely time-locked to the stimulus, the timing of most spikes, even during dynamical motion stimulation, is determined by the refractory period of the neuron and by random membrane potential fluctuations that are not directly related to the stimulus (Kretzberg et al., 2001a; Warzecha et al., 1998).

7.3.2 Coding of Motion Information by Neural Populations

The encoding of stimuli by neuronal populations is a basic operating principle of nervous systems. The number of neurons that constitute such a neuronal population may be very large. However, the population of TCs in the blowfly motion vision system comprises only a relatively small number of 50 to 60 cells in each half of the brain. Each of these cells is thought to encode different aspects of optic flow (see ~~above~~; reviews: Borst and Haag, 2002; Egelhaaf et al., 2002; Hausen and Egelhaaf, 1989; Krapp, 2000). The representation of sensory information by neuronal populations raises the question of the mechanism that eventually decodes this distributed information and uses it to guide behavior. In particular, it is important to assess how well relevant stimulus parameters are preserved in the population response and how specifically these parameters can be extracted by a readout mechanism. Whereas there are only few experimental studies addressing this problem, the constraints that must be taken into account when interpreting neuronal population responses are analyzed theoretically or by model simulations in a wide variety of studies (reviews: Dayan and Abbott, 2001; Oram et al., 1998; Pouget et al., 1998, 2003).

AU: Pls specify where.

Population coding is most frequently analyzed for a bank of sensory neurons encoding a single stimulus parameter. The optimal stimulus of different neurons varies along the stimulus axis. The tuning of an individual cell with respect to this stimulus parameter is usually described by a Gaussian function; that is, the response first increases with changing stimulus parameter, reaches an optimum, and then decreases again. Alternatively, for periodic stimuli axes (e.g., for orientation tuning), harmonic functions, such as cosine functions or truncated cosine functions, are employed to describe tuning curves.

Neural population coding has recently been studied in a subpopulation of blowfly TCs, the so-called VS cells. The ten VS cells in each half of the brain are thought to signal rotations of the head around different axes lying in the equatorial plane of the fly's eye (Krapp et al., 1998). However, VS cell responses are highly ambiguous because they are also activated during upward lift movements of the animal (Karmeier et al., 2003). Even if we assume VS cells to be perfect detectors for self-rotation, their responses are ambiguous due to their cosine-shaped tuning curves and the variability of their responses (Figure 7.8a,d). Assuming a single stimulus dimension (i.e., the orientation of the axis of self-rotation), encoding accuracy of the population of VS cells was determined (Figure 7.8b,f). For each stimulus condition (i.e., for each rotation axis) the activity distribution of all ten VS cells is determined.

Given these response probabilities, the likelihood of a particular rotation axis given a certain response — and, thus, the most likely rotation axis — can be estimated using Bayes's theorem (Dayan and Abbott, 2001). The encoding error is determined from the estimated and the real rotation axis (Figure 7.8c,e,f).

This approach has been applied to VS cells for different rotational velocities and different time windows after the onset of ~~motion~~. Despite the considerable neural noise, the rotation axis can be estimated within ~~5~~ msec with an accuracy of less than 2°. This result is surprising, given the ambiguous responses of individual sensory neurons (Figure 7.8a,b), and it thus stresses the significance of population coding. The decoding performance of VS cells does not improve for larger time windows but deteriorates considerably if only three instead of the ten VS cells are taken into account (Figure 7.8d,e). The finding that a very small time window is sufficient for decoding the orientation axis from the population response has important functional implications for flies, because they perform rapid acrobatic flight maneuvers, which require fast and accurate sensory control signals for visual flight and gaze stabilization (see Chapter 4).

Theoretical studies demonstrate that the accuracy of stimulus encoding depends on a variety of other aspects, such as noise correlation between single elements of the population, the width of the tuning curves, and the number of stimulus dimensions to be encoded (e.g., Abbott and Dayan, 1999; Pouget et al., 1999; Wilke and Eurich, 2001; Zhang and Sejnowski, 1999). These features must be taken into account, although it is far from trivial to obtain the large amount of experimental data required to understand fully the encoding of sensory information by neuronal populations. All these analyses are only first steps toward understanding the encoding of complex natural motion stimuli as experienced by the animals in normal behavioral situations (see next section). This will require the development of novel theoretical approaches to analyze neuronal population data (see also Chapter 5).

7.4 APPROACHES TO INVESTIGATE THE ENCODING OF NATURAL VISUAL STIMULI

Information processing within a neural circuit is traditionally analyzed with stimuli that are much simpler with respect to their spatial and dynamical features than the input an animal encounters in behavioral situations. Because visual systems evolved in specific environments and behavioral contexts, the functional significance of the information being processed can only be assessed by analyzing neuronal performance under conditions that come close to natural situations.

One important aspect applies to the dynamical properties of the optic flow that is encountered during behavior. These are determined by the dynamics of the animal's self-motion and the three-dimensional layout of the environment. The characteristics of the optic flow may differ greatly for different species and in different behavioral situations. Some insects, such as hoverflies, dragonflies, and hawkmoths, are able to hover in midair in front of a flower (Collett and Land, 1975; Farina et al., 1994; Kern and Varjú, 1998). From their current position in space, these insects can accelerate rapidly and dart off at high velocities. Blowflies usually change the

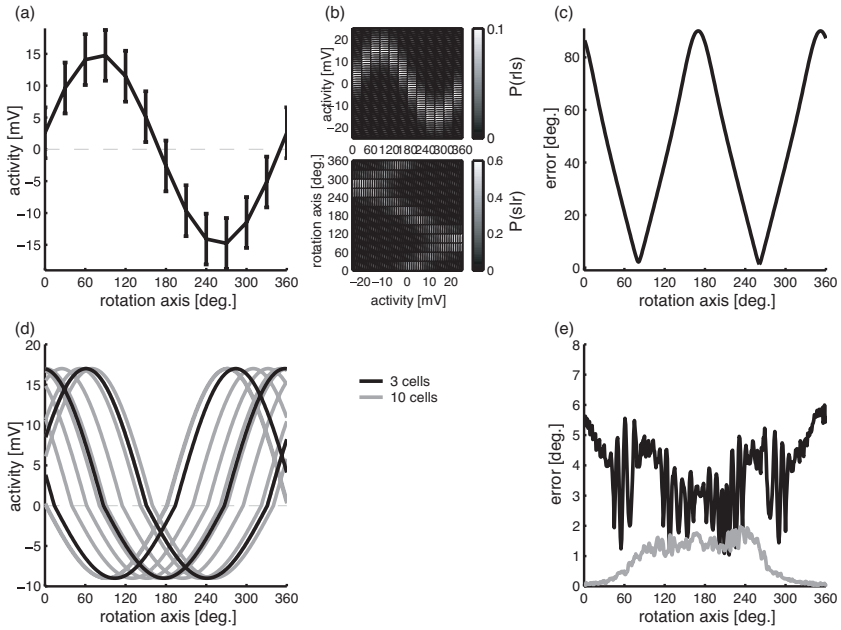

(f)

$\vec{r}$ response vector describing the population response

$p(\vec{r}|s_x)$ *can be measured* probability distribution of the population response to the stimulus s_x

$p(s_x|\vec{r})$ *to be determined* probability of the stimulus s_x given the response vector $\vec{r}$

Applying Bayes Theorem allows determination of $p(s_x|\mathbf{r})$ from measurable data:

$$p(s_x|\vec{r}) = \frac{p(\vec{r}|s_x)\, p(s_x)}{p(\vec{r})}$$

Estimated stimulus for a given population response r: $s_{est} = \sum_{s_x} p(s_x|\vec{r})\, s_x$ Error $\sqrt{(s - s_{est})^2}$

FIGURE 7.8 Accuracy of population coding illustrated for a class of TCs, the ten VS cells. **a**: The response of each VS cell depends on the orientation of an horizontally aligned axis about which a panoramic wide-field pattern is rotated. The tuning can be approximated by a distorted cosine function. **b**: The rotation axis can be estimated from the measured response distributions obtained for the different rotation axes $p(r|s_i)$ (compare Figure 7.5). By applying Bayes's theorem (see **f**), the probability distribution of rotation axes can be determined for a given response $p(s_i|r)$. **c**: The coding error is given by the standard deviation between the estimated orientation axis and the real orientation axis (for formal details see **f**). If the response of only one VS cell is taken into account, the coding error varies strongly with the rotation axis and may assume very large values. **d**: If the responses of more VS cells are taken into account, the coding error decreases to very small values, even if only a 5 msec response interval is used for decoding. Tuning curves of all ten VS cells (gray lines) and a subgroup of three VS cells (black lines). **e**: Corresponding coding errors. **f**: Formal explanation of the decoding procedure.

direction of self-motion rapidly by saccadic turns during flight (van Hateren and Schilstra, 1999) or, one order of magnitude more slowly, while walking (Horn and Mittag, 1980; Kern et al., 2001b). Because the optic flow pattern and its dynamics are species and context specific, it is reasonable to assume that the mechanisms extracting motion information are adapted to behaviorally relevant conditions. Because it is hard to record from visual interneurons in freely moving insects, more indirect approaches have recently been used to determine the responses of motion-sensitive neurons to a variety of approximations to behaviorally generated optic flow.

Recordings of the H1 cell have been made from the brains of blowflies that were oscillated with a turntable with dynamics that mimic the rotational component of flight trajectories of unrestrained small houseflies (Lewen et al., 2001). For technical reasons, the most distinctive feature of optic flow of free-flying blowflies (i.e., the succession of saccadic turns and stable gaze) (van Hateren and Schilstra, 1999) was not taken into account and the angular velocity of the turntable was only half that of the flight trajectory.

In an alternative approach, neural responses were recorded from the brain of tethered moths flying in a flight simulator in which the animal can influence its visual input as under free-flight conditions (Gray et al., 2002). So far, this elegant approach is restricted to relatively large insect species, such as locusts or moths, changing their direction of flight relatively slowly.

In another approach, the optic flow experienced by behaving blowflies was reconstructed and replayed to the animal during nerve cell recordings. This approach has been employed for various behavioral situations during tethered flight in a flight simulator (Kimmerle and Egelhaaf, 2000b; Warzecha and Egelhaaf, 1996, 1997), during unrestrained walking in a three-dimensional environment (Kern et al., 2000, 2001a), and recently during rapid free-flight maneuvers in a three-dimensional environment (Figure 7.9a) (Kern et al., 2001b, 2004~~a, 2004b~~; Lindemann et al., 2003).

The simulation of free flight has become possible thanks to the development of sophisticated techniques. First, free-flight behavior can be monitored by means of magnetic sensor coils mounted on the head and thorax of the animal (van Hateren and Schilstra, 1999; Schilstra and van Hateren, 1999) or by high-speed digital cameras (Oddos et al., 2003). Second, a panoramic visual stimulator (FliMax) for presentation of optic flow has been designed that is sufficiently fast for visual stimuli as experienced by free-flying insects (Figure 7.9a). FliMax is a special-purpose panoramic VGA output device generating image frames at a frequency of 370 Hz (Lindemann et al., 2003). FliMax is composed of printed circuit boards shaped like equilateral triangles (side: 30 cm), assembled to form 14 of the 20 sides of an icosahedron (radius of inscribed sphere: 22.4 cm). Each of these boards supports 512 regularly spaced, round light-emitting diodes, or LEDs (#WU-2-53GD, 5 mm, emitting wavelength: 567 nm, effective viewing angle: 25º).[32] All 7168 LEDs are controlled individually via a computer equipped with a standard VGA graphics card and customized software. The luminance of each LED, adjustable to eight intensity levels, is kept constant between updates by sample-and-hold circuits. FliMax is open toward the back to mount an animal in its center and to make recordings from the blowfly's brain (Lindemann et al., 2003).

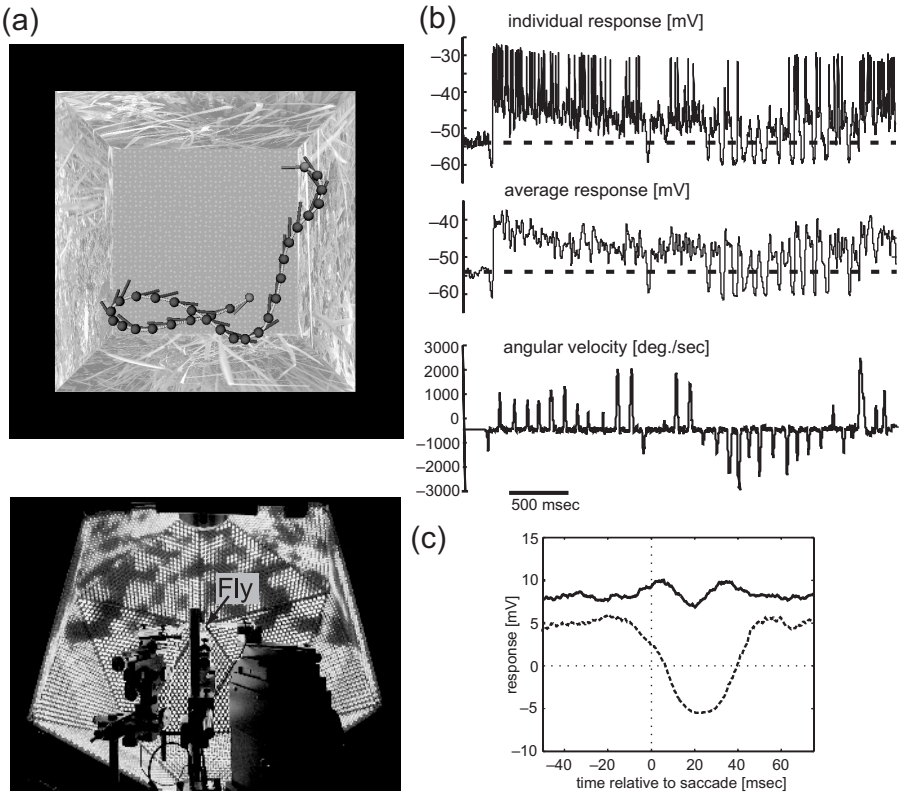

FIGURE 7.9 Responses of the HSE cell of a blowfly to behaviorally generated optic flow as experienced during a free-flight maneuver. **a**: Upper diagram: Flight trajectory as seen from above monitored in a cubic cage ($0.4 \times 0.4 \times 0.4$ m^3) covered on its side walls with images of herbage (for clarity shown only at low contrast). The position of the fly is displayed by small spheres every 10 msec. The position and orientation of the head are shown every 130 msec. Bottom diagram: Photograph of FliMax from behind. In the foreground, the micromanipulators can be seen by which recording electrodes are inserted into the fly's brain. **b**: Responses of an HSE cell in the right half of the visual system to behaviorally generated stimuli. Top trace: Individual response; cell responds to motion with graded de- and hyperpolarizations; spikelike depolarizations superpose the graded potential changes. Second trace: Average response (n = 7). Third trace: Angular velocity of the fly's head. Sharp angular velocity peaks corresponding to saccadelike turns of the fly dominate the time-dependent angular velocity profile. Positive (negative) values denote counterclockwise (clockwise) turns of the head in a head-centered coordinate system. In contrast to expectations based on the input organization of the HSE cell (Figure 7.1a), there are no obvious response peaks during preferred direction motion evoked by counterclockwise saccades. However, there are pronounced hyperpolarizations going along with clockwise saccades. Dotted horizontal lines indicate resting potential. **c**: Saccade-triggered average of the HSE responses. Counterclockwise saccades (solid line) go along with image motion in the HSE cell's preferred direction; clockwise saccades (dotted line) go along with image motion in the null direction. Zero time corresponds to the maximum angular velocity. The resting potential was subtracted before averaging. (Flight trajectory provided by JH van Hateren; Experimental data from Lindemann, J.P. et al., *Vision Res.* **43**:779–791, 2003. With permission.)

Although the analysis of how natural visual stimuli are processed has started only recently, it is already safe to conclude that the neuronal responses to complex optic flow as experienced under behavioral conditions can be understood only partly in terms of the concepts that were established on the basis of experiments done with conventional motion stimuli. This is illustrated in the following example.

In moving animals, retinal image flow is distinguished from conventional (experimenter-designed) visual stimuli by its characteristic dynamics, which are largely determined by the animal's own actions and reactions. During spontaneous flight, blowflies execute a series of saccadic turns where the head shows angular velocity peaks of up to several thousand degrees per second. Between saccades, the gaze is kept basically stable (van Hateren and Schilstra, 1999; Schilstra and van Hateren, 1999). The resulting retinal image flow was reconstructed and replayed to blowflies. The resulting complex time-dependent responses were related by reverse reconstruction approaches (see Section 7.3.1) to various self-motion parameters, such as yaw rotation, forward translation, and sideslip. How well the original self-motion parameters can be estimated from the neuronal responses is quantified by the coherence (see Section 7.3.1). Our results, obtained with natural optic flow on the so-called HSE neuron, do not match conclusions based on systems analysis of the neuron's properties with experimenter-designed stimuli (Kern et al., 2004a):

1. It was previously concluded that the neuron should mainly act as a detector of self-rotation of the animal around its vertical axis (see Figure 7.1). In contrast, our results with behaviorally generated optic flow show that the neuron fails to encode faithfully even the most prominent turns of the animal as found during saccades.
2. Although the cell experiences the largest optic flow during saccades, it may encode behaviorally relevant information, especially between saccades. Between saccades blowflies keep their gaze stable apart from small, broadband yaw rotations, so they may gather useful information about the outside world from the translational optic flow components that dominate at low frequencies in intersaccadic intervals. Indeed, between saccades, neural signals provide rich information about the spatial relation of the animal to its surroundings. It should be noted that distance is signaled only relative to the fly's own velocity, because retinal velocities evoked during translation are inversely proportional to distance and proportional to translation velocity. This implies that in walking flies, the visual surroundings should affect the responses of the HSE cell only when the fly is very close to environmental structures, just as has been found in electrophysiological experiments (Kern et al., 2001a, 2001b). This implicit scaling of distance information by the actual speed of the animal may be a parsimonious and advantageous way to extract from optic flow behaviorally relevant information about the outlay of the environment, because, for instance, evasive actions evoked by obstacles in the path of locomotion need to be evoked only at a smaller distance when the animal moves more slowly.
3. Based on experimenter-designed motion stimuli, motion-sensitive neurons are frequently expected to encode stimulus velocity. Indeed, stimulus

velocity can be reconstructed faithfully from the responses of blowfly motion-sensitive neurons, as long as the velocities and velocity changes are relatively small (Bialek et al., 1991; Egelhaaf and Reichardt, 1987; Haag and Borst, 1997). However, we could show that under behaviorally relevant stimulus conditions, the visual motion system of the blowfly operates far beyond this linear range for a considerable portion of time (Figure 7.9b,c). We concluded that, in contrast to previous views, the nonlinearities of the visual motion system may be essential for the HSE cell to encode information about the spatial relation of the animal to its environment. If the neuron encoded linearly the entire velocity range the system encounters in behavior, by far the largest responses would be generated during body saccades. This would leave only a very small response range for encoding optic flow in the intersaccadic interval. Given the noisiness of neuronal signals (see ~~above~~), it might be difficult to extract meaningful information about the spatial organization of the surroundings from the neuronal responses. Because angular velocities during saccades are far beyond the linear range of the motion detection system, the HSE cell appears to be able to encode useful information about translation and thus about the spatial relation of the animal to the outside world. This finding emphasizes that the significance of neuronal circuits can only be assessed if they are probed in the natural operating range.

AU: Pls specify where.

So far, only the specificity of individual neurons has been analyzed in encoding of behaviorally relevant features from the natural optic flow. With the available techniques, the next step will be to understand how this specificity is increased by taking into account more of the relevant elements of the TC population. This analysis, however, will require the development of novel conceptual and technical approaches to handle the resulting complex time-dependent population data.

7.5 CONCLUSIONS AND OUTLOOK

Thanks to great methodological and conceptual developments, many aspects of the neural computations underlying visually guided orientation behavior in the blowfly have been elucidated in recent years. Analysis has ranged from the biophysical properties of neurons and their synaptic interactions, to the performance and reliability of neural populations in encoding behaviorally relevant motion sequences, to orientation behavior in flight simulators and under free-flight conditions. Accordingly, the employed methodological repertoire is very broad. On the one hand, sophisticated techniques of cellular physiology had to be adapted to *in vivo* conditions — to mention only the imaging of the spatially resolved intracellular activity patterns and, in particular, the time-dependent distribution of ions involved in intracellular information processing. Likewise, thanks to novel compounds such as photolabile calcium cages, targeted manipulation of intracellular ion concentrations could be performed. On the other hand, developments, for instance in computer graphics, have recently allowed for the first time the presentation of natural motion stimuli in electrophysiological experiments, as they were encountered by freely

behaving animals. The complex spatio–temporal properties of natural image sequences and the resulting complex time-dependent neuronal responses have made it necessary to establish and adapt sophisticated techniques for analysis of such complex data structures. Moreover, taking into account the variability of responses of individual neurons and the activity of whole populations of them has made another set of novel approaches to data analysis necessary and neurobiology an increasingly interdisciplinary effort.

Insect model systems, such as the visual motion pathway of the blowfly, are particularly advantageous for this multifaceted interdisciplinary effort. Experimental analysis down to the biophysical level can be done *in vivo,* where the system can be probed with behaviorally generated input and, thus, under its natural operating conditions. Because populations of neurons are relatively small compared to those of mammals, it appears to be possible to boil down visually guided behavior to the computational properties of neural networks of identified neurons. Despite the small size of insects' brains, these computations are far from trivial, given the fact that many insects, such as blowflies, are able to perform extraordinary things — at least when compared to autonomous manmade machines. Hence, disclosing computational design principles of insect brains down to the level of neurons and neural networks is not only one of the most fascinating missions of basic science, but also a strategic goal if robots with autonomous behavior are to be realized (see Chapter 8). To test the viability of biologically established computational principles, but also to translate these principles into a language that can be implemented in artificial systems, modeling is an indispensable tool. Indeed, in all laboratories investigating blowfly vision, modeling was intensively employed in parallel with experimental analysis at all levels, ranging from computations of single cells to overall behavioral performance (reviews: Borst, 2003; Egelhaaf et al., 2003).

Finally, it should be mentioned that because of the efficiency of visually guided orientation behavior in insects, there is great interest in applying principles of insect motion information processing to autonomous artificial systems (see Chapter 8). Although this has been successful for some behavioral components (~~Franz and Mallot, 2000;~~ Harrison and Koch, 2000; Huber et al., 1999; Rind, 2002; Srinivasan et al., 1997, 2001), biomorphic autonomous robots still appear to be dull compared with the original after which they are modeled. In contrast to manmade systems, natural vision systems have been tested and improved on a much longer timescale by many millions of years of evolution.

ACKNOWLEDGMENTS

The work in the authors' laboratory is supported by the Deutsche Forschungsgemeinschaft (DFG).

REFERENCES

Abbott LF, Dayan P (1999) The effect of correlated variability on the accuracy of a population code. *Neural Computation* **11**:91–101.

Barberini CL, Horwitz GD, Newsome WT (2000) A comparison of spiking statistics in motion sensing neurons of flies and monkeys. In: *Computational, Neural and Ecological Constraints of Visual Motion Processing*. Zanker JM, Zeil J, Eds., Springer, Heidelberg, pp. 307–320.

Bendat JS, Piersol AG (2000) *Random Data: Analysis and Measurement Procedures.* Wiley-Interscience, New York.

Bialek W, Rieke F, de Ruyter van Steveninck R, Warland D (1991) Reading a neural code. *Science* **252**:1854–1857.

Boeddeker N, Egelhaaf M (2003a) Steering a model fly: simulations on visual pursuit in blowflies. *Proc. R. Soc. Lond. B* **270**:1971–1978.

Boeddeker N, Egelhaaf M (2003b) Chasing behaviour of blowflies: a smooth pursuit system generates saccades. (submitted)

AU: Pls update.

Boeddeker N, Kern R, Egelhaaf M (2003) Chasing a dummy target: smooth pursuit and velocity control in male blowflies. *Proc. R. Soc. Lond. B* **270**:393–399.

Borst A, Haag J (2001) Effects of mean firing on neural information rate. *J. Comput. Neurosci.* **10**:213–221.

Borst A, Haag J (2002) Neural networks in the cockpit of the fly. *J. Comp. Physiol. A* **188**:419–437.

Borst A, Theunissen FE (1999) Information theory and neural coding. *Nature Neurosci.* **2**:947–957.

Collett TS (1971) Visual neurones for tracking moving targets. *Nature* **232**:127–130.

Collett TS, Land MF (1975) Visual control of flight behaviour in the hoverfly *Syritta pipiens* L. *J. Comp. Physiol.* **99**:1–66.

Dayan P, Abbott LF (2001) *Theoretical Neuroscience: Computational and Mathematical Modeling of Neural Systems*. MIT Press, Cambridge, MA.

Egelhaaf M (1985a) On the neuronal basis of figure–ground discrimination by relative motion in the visual system of the fly. II. Figure-detection cells, a new class of visual interneurones. *Biol. Cybern.* **52**:195–209.

Egelhaaf M (1985b) On the neuronal basis of figure–ground discrimination by relative motion in the visual system of the fly. III. Possible input circuitries and behavioural significance of the FD-cells. *Biol. Cybern.* **52**:267–280.

Egelhaaf M, Borst A, Warzecha A-K, Flecks S, Wildemann A (1993) Neural circuit tuning fly visual interneurons to motion of small objects. II. Input organization of inhibitory circuit elements by electrophysiological and optical recording techniques. *J. Neurophysiol.* **69**:340–351.

Egelhaaf M, Kern R (2002) Vision in flying insects. *Curr. Opin. Neurobiol.* **12**:699–706.

Egelhaaf M, Kern R, Kurtz R, Krapp HG, Kretzberg J, Warzecha A-K (2002) Neural encoding of behaviourally relevant motion information in the fly. *Trends Neurosci.* **25**:96–102.

Egelhaaf M, Reichardt W (1987) Dynamic response properties of movement detectors: theoretical analysis and electrophysiological investigation in the visual system of the fly. *Biol. Cybern.* **56**:69–87.

Egelhaaf M, Warzecha A-K (1999) Encoding of motion in real time by the fly visual system. *Curr. Opin. Neurobiol.* **9**:454–460.

Esch HE, Burns JM (1996) Distance estimation by foraging honeybees. *J. Exp. Biol.* **199**:155–162.

Esch HE, Zhang S, Srinivasan MV, Tautz J (2001) Honeybee dances communicate distances measured by optic flow. *Nature* **411**:581–583.

Farina WM, Varjú D, Zhou Y (1994) The regulation of distance to dummy flowers during hovering flight in the hawk moth *Macroglossum stellatarum. J. Comp. Physiol.* **174**:239–247.

Farrow K, Haag J, Borst A (2003) Input organization of multifunctional motion-sensitive neurons in the blowfly. *J. Neurosci.* **29**:9805–9811.

Fortune ES, Rose GJ (2001) Short-term synaptic plasticity as a temporal filter. *Trends Neurosci.* **24:**381–385.

~~Franz MO, Mallot HA (2000) Biomimetic robot navigation. *Robots and Autonomous Systems* 133–153. [volume #?]~~

AU: Pls supply.

Gauck V, Borst A (1999) Spatial response properties of contralateral inhibited lobula plate tangential cells in the fly visual system. *J. Comp. Neurol.* **406**:51–71.

Gilbert C, Strausfeld NJ (1991) The functional organization of male-specific visual neurons in flies. *J. Comp. Physiol. A* **169**:395–411.

Gray JR, Pawlowski VM, Willis MA (2002) A method for recording behavior and multineuronal CNS activity from tethered insects flying in virtual space. *J. Neurosci. Meth.* **120**:211–223.

Grewe J, Kretzberg J, Warzecha A-K, Egelhaaf M (2003) Impact of photon-noise on the reliability of a motion-sensitive neuron in the fly's visual system. *J. Neurosci.* **23**:10776–10783.

Haag J, Borst A (1997) Encoding of visual motion information and reliability in spiking and graded potential neurons. *J. Neurosci.* **17**:4809–4819.

Haag J, Borst A (1998) Active membrane properties and signal encoding in graded potential neurons. *J. Neurosci.* **18**:7972–7986.

Haag J, Borst A (2001) Recurrent network interactions underlying flow-field selectivity of visual interneurons. *J. Neurosci.* **21**:5685–5692.

Haag J, Borst A (2002) Dendro-dendritic interactions between motion-sensitive large-field neurons in the fly. *J. Neurosci.* **22**:3227–3233.

Haag J, Borst A (2003) Orientation tuning of motion-sensitive neurons shaped by vertical-horizontal network interactions. *J. Comp. Physiol. A* **189**:363–370.

Harrison RR, Koch C (2000) A silicon implementation of the fly's optomotor control system. *Neural Comput.* **12**:2291–2304.

Hateren JH van, Schilstra C (1999) Blowfly flight and optic flow. II. Head movements during flight. *J. Exp. Biol.* **202**:1491–1500.

Hateren JH van, Snippe HP (2001) Information theoretical evaluation of parametric models of gain control in blowfly photoreceptor cells. *Vision Res.* **41**:1851–1865.

Hausen K (1981) Monocular and binocular computation of motion in the lobula plate of the fly. *Verh. Dtsch. Zool. Ges.* **74**:49–70.

Hausen K, Egelhaaf M (1989) Neural mechanisms of visual course control in insects. In: *Facets of Vision.* Stavenga D, Hardie RC, Eds., Springer, Berlin, pp. 391–424.

Hengstenberg R (1982) Common visual response properties of giant vertical cells in the lobula plate of the blowfly *Calliphora*. *J. Comp. Physiol.* **149**:179–193.

Horn E, Mittag J (1980) Body movements and retinal pattern displacements while approaching a stationary object in the walking fly, *Calliphora erythrocephala*. *Biol. Cybern.* **39**:67–77.

Horstmann W, Egelhaaf M, Warzecha A-K (2000) Synaptic interactions increase optic flow specificity. *Eur. J. Neurosci.* **12**:2157–2165.

Huber SA, Franz MO, Bülthoff HH (1999) On robots and flies: modeling the visual orientation behavior of flies. *Robotics and Autonomous Systems* **29**:227–242.

Juusola M, French AS, Uusitalo RO, Weckström M (1996) Information processing by graded-potential transmission through tonically active synapses. *Trends Neurosci*. **19**:292–297.

Kalb J, Nielsen T, Fricke N, Egelhaaf M, Kurtz R (2004) *In vivo* two-photon laser-scanning microscopy of Ca^{2+} dynamics in visual motion-sensitive neurons. *Biochem. Biophys. Res. Communic.* **316**:341–347.

Karmeier K, Egelhaaf M, Krapp HG (2001) Early visual experience and receptive field organization of the optic flow processing interneurons in the fly motion pathway. *Vis. Neurosci.* **18**:1–8.

Karmeier K, Krapp HG, Egelhaaf M (2003) Robustness of the tuning of fly visual interneurons to rotatory optic flow. *J. Neurophysiol*. **90**:1626–1634.

Kern R, van Hateren JH, Michaelis C, Lindemann JP, Egelhaaf M (2004~~a~~) Eye movements during natural flight shape the function of a blowfly motion sensitive neuron. (submitted).

AU: Pls update.

Kern R, Lutterklas M, Egelhaaf M (2000) Neural representation of optic flow experienced by unilaterally blinded flies on their mean walking trajectories. *J. Comp. Physiol. A* **186**:467–479.

Kern R, Lutterklas M, Petereit C, Lindemann JP, Egelhaaf M (2001a) Neuronal processing of behaviourally generated optic flow: experiments and model simulations. *Network: Computations in Neural Systems* **12**:351–369.

~~Kern R, Oddos F, Schwerdtfeger G, Egelhaaf M (2004b) Performance of fly H1 neuron during free-flight. (submitted).~~

AU: Pls update.

Kern R, Petereit C, Egelhaaf M (2001b) Neural processing of naturalistic optic flow. *J. Neurosci.* **21**:1–5.

Kern R, Varjú D (1998) Visual position stabilization in the hummingbird hawk moth, *Macroglossum stellatarum* L.: I. Behavioural analysis. *J. Comp. Physiol. A* **182**:225–237.

Kimmerle B, Egelhaaf M (2000a) Detection of object motion by a fly neuron during simulated translatory flight. *J. Comp. Physiol. A* **186**:21–31.

Kimmerle B, Egelhaaf M (2000b) Performance of fly visual interneurons during object fixation. *J. Neurosci.* **20**:6256–6266.

Koenderink JJ (1986) Optic flow. *Vis. Res.* **26**:161–180.

Krapp HG (2000) Neuronal matched filters for optic flow processing in flying insects. In: *Neuronal Processing of Optic Flow.* Lappe M, Ed., Academic Press, San Diego, CA, pp. 93–120.

Krapp HG, Hengstenberg B, Hengstenberg R (1998) Dendritic structure and receptive-field organization of optic flow processing interneurons in the fly. *J. Neurophysiol.* **79**:1902–1917.

Krapp HG, Hengstenberg R (1996) Estimation of self-motion by optic flow processing in single visual interneurons. *Nature* **384**:463–466.

Krapp HG, Hengstenberg R, Egelhaaf M (2001) Binocular contribution to optic flow processing in the fly visual system. *J. Neurophysiol.* **85**:724–734.

Kretzberg J, Egelhaaf M, Warzecha A-K (2001a) Membrane potential fluctuations determine the precision of spike timing and synchronous activity: a model study. *J. Comput. Neurosci.* **10**:79–97.

Kretzberg J, Warzecha A-K, Egelhaaf M (2001b) Neural coding with graded membrane potential changes and spikes. *J. Comput. Neurosci.* **11**:153–164.

Kurtz R (2004) Ca^{2+} clearance in visual motion-sensitive neurons of the fly studied *in vivo* by sensory stimulation and UV photolysis of caged Ca^{2+}. ~~(submitted).~~

AU: Pls update.

Kurtz R, Egelhaaf M (2003) Natural patterns of neural activity. *Molecular Neurobiol.* **27**:1–19.

Kurtz R, Warzecha A-K, Egelhaaf M (2001) Transfer of visual information via graded synapses operates linearly in the natural activity range. *J. Neurosci.* **21**:6957–6966.

Land MF, Collett TS (1974) Chasing behaviour of houseflies (*Fannia canicularis*): a description and analysis. *J. Comp. Physiol.* **89**:331–357.

Lappe M (2000) *Neuronal Processing of Optic Flow*. Academic Press, San Diego, CA.

Lewen GD, Bialek W, de Ruyter van Steveninck R (2001) Neural coding of naturalistic stimuli. *Network: Comput. Neural Syst.* **12**:317–329.

Lindemann JP, Kern R, Michaelis C, Meyer P, van Hateren JH, Egelhaaf M (2003) FliMax, a novel stimulus device for panoramic and high-speed presentation of behaviourally generated optic flow. *Vision Res.* **43**:779–791.

Marmarelis PZ, Marmarelis VZ (1978) *Analysis of Physiological Systems*. Plenum Press, New York.

Miller JP, Selverston AI (1979) Rapid killing of single neurons by irradiation of intracellularly injected dye. *Science* **206**:702–704.

Neher E (1998) Vesicle pools and Ca^{2+} microdomains: new tools for understanding their roles in neurotransmitter release. *Neuron* **20**:389–399.

Oddos F, Kern R, Boeddeker N, Egelhaaf M (2003) Flight performance modified by environmental changes in the blowfly Lucilia. In: *Göttingen Neurobiology Report*. Elsner N, Ed., Georg Thieme, Stuttgart, p. 444.

Olberg RM (1981) Object- and self-movement detectors in the ventral nerve cord of the dragonfly. *J. Comp. Physiol.* **141**:327–334.

Olberg RM (1986) Identified target-selective visual interneurons descending from the dragonfly brain. *J. Comp. Physiol.* **159**:827–840.

Olberg RM, Pinter RB (1990) The effect of mean luminance on the size selectivity of identified target interneurons in the dragonfly. *J. Comp. Physiol. A* **166**:851–856.

Oram MW, Földiák P, Perrett DI, Sengpiel F (1998) The "ideal homunculus": decoding neural population signals. *Trends Neurosci.* **21**:259–265.

Paulsen O, Sejnowski TJ (2000) Natural patterns of activity and long-term synaptic plasticity. *Curr. Opin. Neurobiol.* **10**:172–179.

Pouget A, Dayan P, Zemel RS (2003) Inference and computation with population codes. *Ann. Rev. Neurosci.* **26**:381–410.

Pouget A, Deneve S, Ducom J-C, Latham PE (1999) Narrow versus wide tuning curves: what's best for a population code? *Neural Comput.* **11**:85–90.

Pouget A, Zhang K, Deneve S, Latham PE (1998) Statistically efficient estimation using population coding. *Neural Comput.* **10**:373–401.

Rieke F, Warland D, de Ruyter van Steveninck R, Bialek W (1997) *Spikes: Exploring the Neural Code*. MIT Press, Cambridge, MA.

Rind FC (2002) Motion detectors in the locust visual system: from biology to robot sensors. *Microsc. Res. Tech.* **56**:256–269.

Rind FC, Simmons PJ (1999) Seeing what is coming: building collision-sensitive neurones. *Trends Neurosci.* **22**:215–220.

Ruyter van Steveninck R de, Lewen GD, Strong SP, Koberle R, Bialek W (1997) Reproducibility and variability in neural spike trains. *Science* **275**:1805–1808.

Sabatini BL, Regehr WG (1999) Timing of synaptic transmission. *Annu. Rev. Physiol.* **61**:521–542.

Schilstra C, van Hateren JH (1999) Blowfly flight and optic flow. I. Thorax kinematics and flight dynamics. *J. Exp. Biol.* **202**:1481–1490.

Simmons, PJ (2002) Signal processing in a simple visual system: the locust ocellar system and its synapses. *Microsc. Res. Tech.* **56**:270–280.

Srinivasan MV, Chahl JS, Zhang SW (1997) Embodying natural vision into machines. In: *From Living Eyes to Seeing Machines*. Srinivasan MV, Venkatesh S, Eds., Oxford University Press, Oxford, pp. 249–265.

Srinivasan MV, Zhang S, Altwein M, Tautz J (2000) Honeybee navigation: nature and calibration of the "odometer." *Science* **287**:851–853.

Srinivasan MV, Zhang S, Chahl JS (2001) Landing strategies in honeybees, and possible applications to autonomous airborne vehicles. *Biol. Bull.* **200**:216–221.

Thomson AM (2000) Facilitation, augmentation and potentiation at central synapses. *Trends Neurosci.* **23**:305–312.

Victor JD, Purpura K (1996) Nature and precision of temporal coding in visual cortex: a metric-space analysis. *J. Neurophysiol.* **76**:1310–1326.

Wagner H (1986) Flight performance and visual control of the flight of the free-flying housefly (*Musca domestica*). II. Pursuit of targets. *Phil. Trans. R. Soc. Lond. B* **312**:553–579.

Warzecha A-K, Egelhaaf M (1996) Intrinsic properties of biological motion detectors prevent the optomotor control system from getting unstable. *Phil. Trans. R. Soc. Lond. B* **351**:1579–1591.

Warzecha A-K, Egelhaaf M (1997) How reliably does a neuron in the visual motion pathway of the fly encode behaviourally relevant information? *Europ. J. Neurosci.* **9**:1365–1374.

Warzecha A-K, Egelhaaf M (1999) Variability in spike trains during constant and dynamic stimulation. *Science* **283**:1927–1930.

Warzecha A-K, Egelhaaf M, Borst A (1993) Neural circuit tuning fly visual interneurons to motion of small objects. I. Dissection of the circuit by pharmacological and photoinactivation techniques. *J. Neurophysiol.* **69**:329–339.

Warzecha A-K, Kretzberg J, Egelhaaf M (1998) Temporal precision of the encoding of motion information by visual interneurons. *Curr. Biol.* **8**:359–368.

Warzecha A-K, Kretzberg J, Egelhaaf M (2000) Reliability of a fly motion-sensitive neuron depends on stimulus parameters. *J. Neurosci.* **20**:8886–8896.

Warzecha A-K, Kurtz R, Egelhaaf M (2003) Synaptic transfer of dynamical motion information between identified neurons in the visual system of the blowfly. *Neurosci.* **119**:1103–1112.

Wehner R (1981) Spatial vision in arthropods. In: *Handbook of Sensory Physiology. Vol. VII/6C: Comparative Physiology and Evolution of Vision in Invertebrates.* Autrum H, Ed., Springer, Berlin, pp. 287–616.

Wilke SD, Eurich CW (2001) Representational accuracy of stochastic neural populations. *Neural Comput.* **14**:155–189.

Zhang K, Sejnowski TJ (1999) Neuronal tuning: to sharpen or broaden? *Neural Comput.* **11**:75–84.